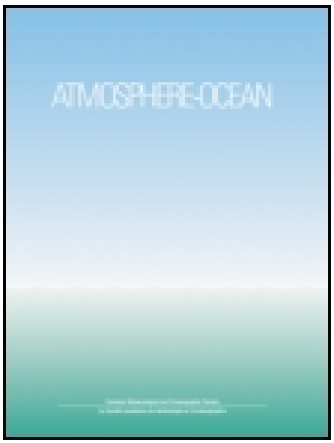

Atmosphere-Ocean

Publication details, including instructions for authors and subscription information:
http://www.tandfonline.com/loi/tato20

An Overview of Numerical Methods for the Next Generation U.K. NWP and Climate Model

M. J.P. Cullen [a], T. Davies [a], M. H. Mawson [a], J. A. James [a], S. C. Coulter [a] & A. Malcolm [b]

[a] Meteorological Office, London Road, Bracknell, Berks., U.K.

[b] Department of Mathematics, University of Reading, Whiteknights, Reading, U.K.

Published online: 26 Jul 2011.

To cite this article: M. J.P. Cullen, T. Davies, M. H. Mawson, J. A. James, S. C. Coulter & A. Malcolm (1997) An Overview of Numerical Methods for the Next Generation U.K. NWP and Climate Model, Atmosphere-Ocean, 35:sup1, 425-444, DOI: 10.1080/07055900.1997.9687359

To link to this article: http://dx.doi.org/10.1080/07055900.1997.9687359

An Overview of Numerical Methods for the Next Generation U.K. NWP and Climate Model

M.J.P. Cullen, T. Davies, M.H. Mawson, J.A. James and S.C. Coulter
Meteorological Office
London Road, Bracknell, Berks., U.K.

and

A. Malcolm
Department of Mathematics,
University of Reading,
Whiteknights, Reading, U.K.

[Original manuscript received 1 November 1994; in revised form 31 July 1995]

ABSTRACT *The U.K. Meteorological Office now uses a single model for atmospheric simulation and forecasting from all scales from mesoscale to climate. The constraints which numerical methods for such a model have to satisfy are described. A new version of the model is being developed with the aims of improving its accuracy by better treatment of the 'balanced' part of the flow, and increasing its applicability by including non-hydrostatic effects. Unusual features of this version are the use of the Charney-Phillips grid in the vertical, to improve the geostrophic adjustment properties, and the method of constructing the semi-implicit algorithm for solving the fully compressible equations. Idealized tests of these two aspects of the scheme are presented, showing that the Charney-Phillips grid reduces spurious gravity wave generation without compromising the treatment of the atmospheric boundary layer, and that the semi-implicit integration scheme can give stable solutions without the need for added temporal diffusion.*

RÉSUMÉ *Le Bureau météorologique du Royaume-Uni utilise maintenant un seul modèle pour la simulation et la prévision atmosphérique, de la mésoéchelle à l'échelle climatique. On décrit les contraintes que les méthodes numériques employées dans un tel modèle doivent satisfaire. On est à élaborer une nouvelle version du modèle qui devrait améliorer sa précision par un meilleur traitement de la partie « équilibrée » de l'écoulement et par une augmentation de son applicabilité, en incluant les effets non hydrostatiques. Cette version possède des caractéristiques inhabituelles, telles que la grille Charney-Phillips dans la verticale pour améliorer les propriétés d'ajustement géostrophique, et la méthode de contruire l'algorithme semi-implicite pour solutionner les équations entièrement compressibles. On présente des essais théoriques des deux aspects du schéma qui montrent que la grille Charney-Phillips réduit la génération d'ondes de gravité non essentielles sans compromettre le traitement de la couche limite atmosphérique et que le schéma d'intégration semi-implicite peut donner des solutions stables sans la nécessité d'ajouter une diffusion temporelle.*

1 Introduction

The U.K. Meteorological Office has used the same atmospheric model for all forecasting and climate simulation applications since 1992 (Cullen, 1993). This is both a result of the need to provide a large range of forecast and advisory services efficiently, and also because of the belief that the same scientific methods of simulating atmospheric behaviour will be appropriate regardless of the application. The need for such 'universal methods' is widely recognized and is even more essential when considering models which have large resolution variation within a single run, such as the stretched grid Action de Recherche Petite Echelle Grande Echelle (ARPEGE) system used operationally by Météo-France and the European Centre for Medium-Range Forecasts (Courtier and Geleyn, 1988).

In this paper we discuss the numerical methods used in this 'unified' model. We initially summarize the methods used in the first version of the model, and the reasons for the choices. Though the model was introduced operationally in 1991–2, the choices of formulation to be used had to be largely finalized in 1989. Since then, there has been a great deal of development of improved numerical algorithms. An example is the greatly increased acceptance of the semi-Lagrangian method for treatment of advection. In this paper we therefore discuss the numerical techniques proposed for the next major upgrade of the 'unified' model. The two main themes are, seeking improved model performance by more accurate treatment of the balanced part of the flow, and increasing the applicability of the model to small scales by including non-hydrostatic effects. The resulting design is described in Sections 3 and 4, and idealized tests of some aspects of it are illustrated in Section 5.

2 The current unified model integration scheme

Any integration scheme used for a forecast model has to be very efficient, because timeliness is a key factor, and the benefits of high horizontal and vertical resolution have been frequently demonstrated. In climate modelling, accuracy at low resolution is very important. Conservation properties are also desirable, both to ensure satisfactory long-term integration behaviour, and to allow proper studies of the thermodynamic and energy budgets from control and perturbation runs in climate change experiments. The integration scheme used in the initial version of the unified model was chosen to be as close to the existing methods used in the U.K. Meteorological Office as possible, while meeting the above requirements. Thus the model used finite difference methods, with a latitude-longitude grid. The algorithm was based on the very efficient split-explicit scheme of Gadd (1978) which was already used for global and limited area forecasting. This was adapted to meet climate model requirements by making it conservative. The key steps were to compute the gravity wave terms, including vertical advection of a basic state potential temperature profile, in short time steps, and using the average mass-weighted velocity from the short time steps in calculating the advection terms. Time-smoothing is applied to the fields within the sequence of short time steps. The advection terms

are approximated by a two step second or fourth order Heun scheme. The method is described in detail by Cullen and Davies (1991). Fourier filtering is used to keep the model stable at high latitudes. This is done conservatively by filtering mass-weighted increments to the thermodynamic variables and mass-weighted velocity fields. A conservative diffusion term is used to remove small scale noise. The use of a deformation dependent nonlinear diffusion scheme of the form $\frac{1}{\mu}\nabla\cdot\mu K(u)\nabla$, where μ is a mass-weighting term, was found to be insufficiently scale selective for use at low resolution, and a scale selective form $(\frac{1}{\mu}\nabla\cdot\mu\nabla)^n$, where n is usually chosen to be 2 or 3, was used instead. In order to increase the accuracy, particularly of global climate integrations, the more accurate form of the primitive equations discussed by White and Bromley (1995) was used.

The performance of the combined advection, diffusion and filtering scheme is illustrated on one of the test problems introduced by Williamson et al. (1992). The fourth order approximation to advection is used. The advection scheme used on its own generates large oscillations if the advecting velocity is not parallel to a line of latitude, but it is the combination of the schemes that is actually approximating the transport in the full numerical model. Figure 1 compares the performance of the scheme with the alternative of using a 'monotone' advection scheme (Morton and Sweby, 1987), and a semi-Lagrangian advection scheme (Bates et al., 1990) where the advecting velocity is at an angle of 15°N to the lines of latitude. A 96 × 73 grid has been used. Both the unified model scheme (Fig. 1a) and the semi-Lagrangian scheme (Fig. 1c) produce overshoots, as indicated by the oscillations in the 1000 contour. Those produced by the unified model scheme are more coherent as expected from the consistent phase error for short wavelengths. The monotone scheme (Fig. 1b) produces no overshoots. The unified model scheme performs better than the others in retaining peak amplitude, but is the worst in the distortion of the shape. Figure 2 shows the variation of the r.m.s. error with diffusion coefficient. Note that the error for the optimum range of diffusion coefficient is lower than that given by the monotone scheme. The unified model scheme requires a time step much lower than that required for linear stability. However, when the scheme is used in the complete model, dispersion of noise by gravity waves allows the full expected time step to be used and there is no evidence that the performance is significantly improved by reducing the time step below the value needed for stability. The use of the fourth order Heun scheme is essential to obtain results of this quality in the test problem. However, the sensitivity of the complete model to the choice between second and fourth order schemes at forecast resolutions (grid lengths less than 100 km) has been slight.

The performance of the unified model is found to be remarkably insensitive to horizontal resolution in many respects. Figure 3 illustrates the simulation of the southern hemisphere circumpolar jet from 10 year integrations using 96 × 73 and 288 × 217 grids as compared with a climatology derived from U.K. operational analyses. Many other large scale aspects of the model performance, such as the zonal mean temperature cross-sections, are similarly insensitive. This suggests that

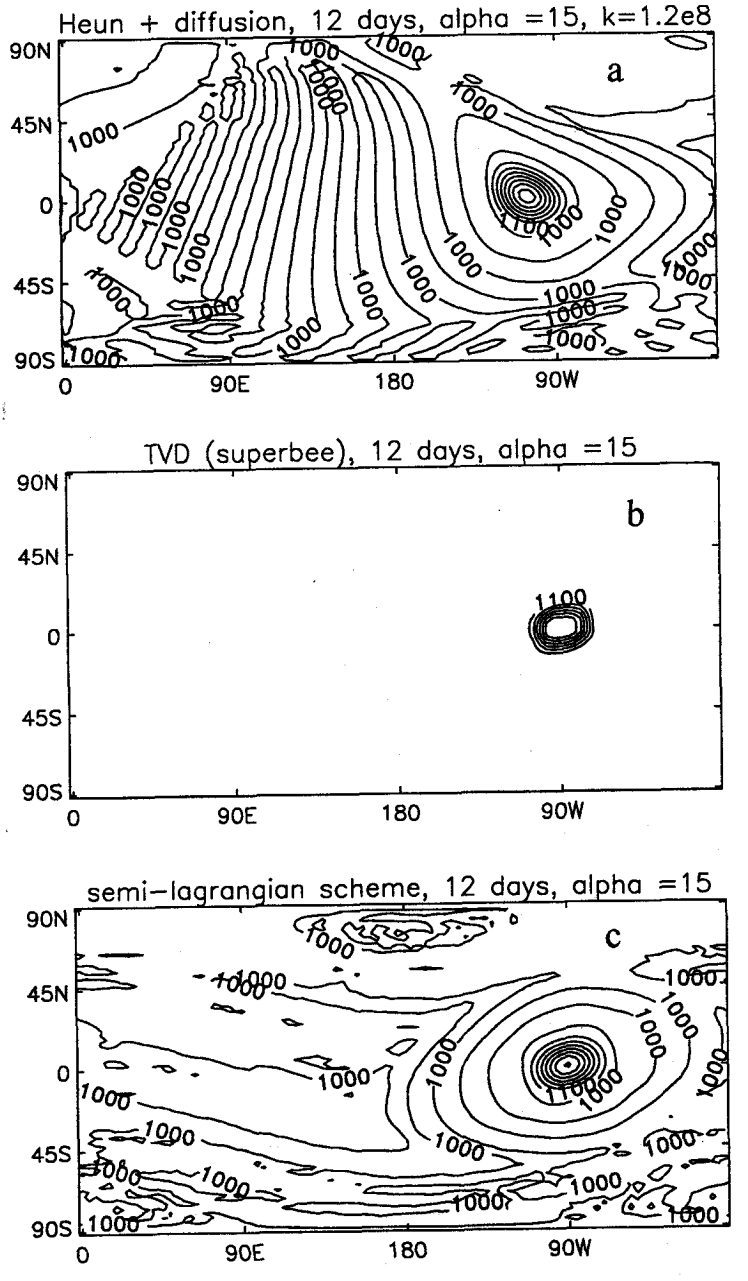

Fig. 1 Solutions for advecting a cosine bell once round a sphere at an angle of 15° to the equator. The initial maximum value is 2000 units. (a) Fourth order Heun scheme with Fourier filtering and fourth order Laplacian diffusion, coefficient 1.2×10^8. (b) Total Variation Diminishing (TVD) scheme with Superbee limiter. (c) Semi-Lagrangian scheme.

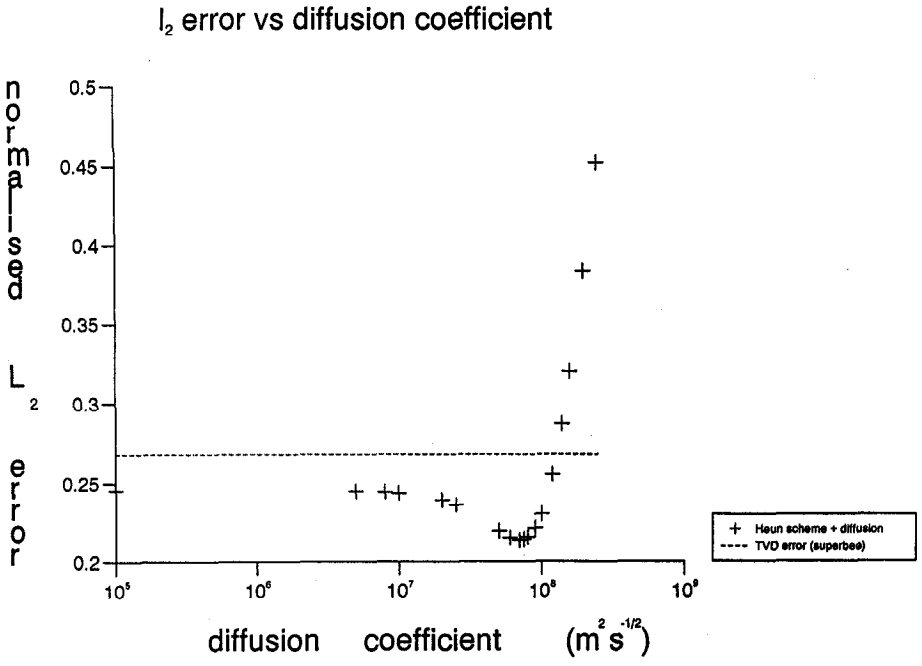

Fig. 2 Root mean square error after one revolution using different diffusion coefficients in the problem of Fig. 1. The dotted line indicates the error of the Superbee scheme.

in seeking further improvements to the model performance it is necessary to review the numerical methods and the physical parametrizations, as well as increasing the resolution further to allow more detail to be simulated.

3 Issues for the proposed new integration scheme

a *Overall requirements*

The purpose of the new scheme is to improve the performance of the model and to increase its scope by including non-hydrostatic effects. Noting the limited sensitivity of the high resolution versions of the model to the simulation of advection, a major attempt is made to improve the simulation of the balanced part of the flow, in particular of the geostrophic adjustment process. As well as improving the model's performance in forecast mode, it is hoped that the performance of the data assimilation will be improved, since much forecast error results from inaccurate analyses. Both requirements lead to the use of semi-implicit integration schemes. It is then natural to consider the use of semi-Lagrangian advection. This allows the maximum time step to be used commensurate with accuracy, and as illustrated in Section 2, reduces distortion of the advection when the flow is not aligned with the grid. There have been doubts about the accuracy of semi-Lagrangian methods when applied in low resolution models. However, the detailed investigation reported by

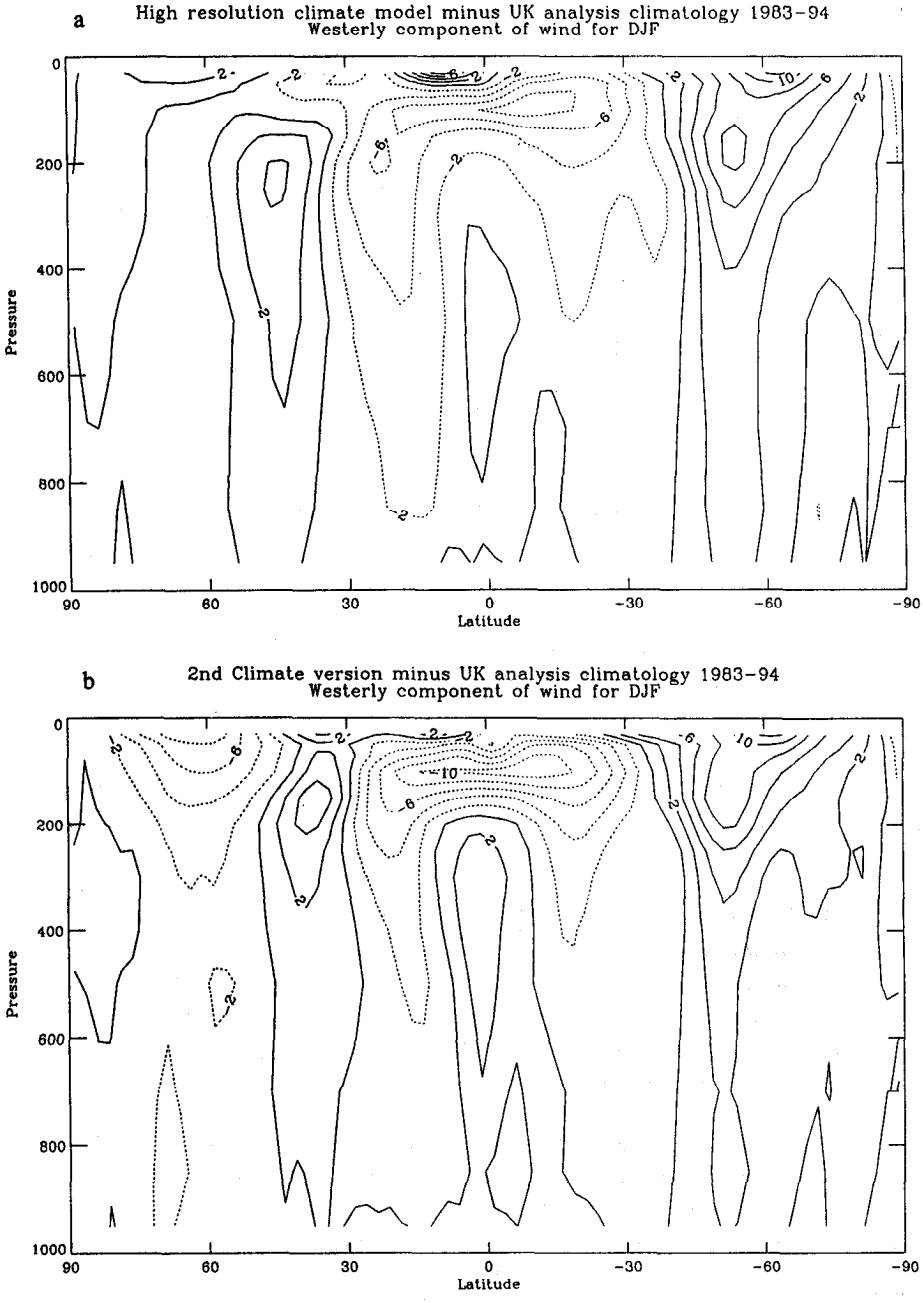

Fig. 3 Cross-section of the difference in zonal wind between multiyear climate model integrations and climatology obtained from U.K. Meteorological Office analyses. (a) High resolution, 288 × 217 grid. (b) Standard resolution 96 × 73 grid.

Williamson and Olson (1994) shows that these losses in accuracy have resulted from using insufficiently accurate interpolation procedures within the method, usually in order to save computer time. In addition, it has been shown, for instance by Priestley (1993), that it is possible to modify the methods so that they satisfy the conservation properties important for climate modelling.

b *Treatment of balanced flow*

There has been considerable study of the finite difference treatment of the geostrophic adjustment process using the shallow water equations, for instance Arakawa and Lamb (1977). This shows that, for non-time-staggered schemes and provided the grid length is less than the Rossby radius of deformation, the 'C' grid arrangement of variables is best, followed by the 'B' grid. Schemes based on vorticity and divergence are at least as good in this respect. There has been much less study of the appropriate treatment of variables in the vertical, because of the tendency to think of a three-dimensional model as a set of shallow water models generated by a decomposition into vertical eigenmodes. However, recent studies such as Arakawa and Moorthi (1987) and Leslie and Purser (1992) have shown that the geostrophic adjustment properties of the 'Charney-Phillips' vertical arrangement of variables are superior to those of the 'Lorenz' arrangement, Fig. 4. This is illustrated by the problem, important in data assimilation, of calculating height increments to balance wind increments. Figure 5 illustrates the error made if we convert wind increments to geostrophically consistent height increments, using a best fitting algorithm on the Lorenz grid, and then recalculating the wind increments geostrophically from the height increments (P. Andrews, private communication). Errors of up to 50% result. On the Charney-Phillips grid this process can be carried out without error.

Though the use of the 'C' grid is well established in finite difference models, the Charney-Phillips grid has been unfashionable recently. One exception is the new Canadian regional model (Tanguay et al., 1990). The reasons are the difficulty of ensuring energy conservation, important in climate modelling, and the more awkward interface to the physics calculations because different variables are held at different places in the vertical column. In particular, the calculations within the boundary layer parametrization may require extra averaging. A method of solving the energy conservation problem is described below and idealized tests of the boundary layer representation are illustrated in Section 5.

Cullen (1989) described and validated numerical methods for the semi-geostrophic equations in a vertical cross-section. This work should be a guide to other aspects of numerical methods important in treating balanced flow accurately. The use of the Charney-Phillips vertical grid was found essential to obtain stable results. Because the equations were implicit in some variables, a semi-implicit method had to be used. Within the method an elliptic equation for a pressure correction was derived and solved, and the results substituted back to complete the update of the other variables. It was necessary to use flow dependent coefficients in the

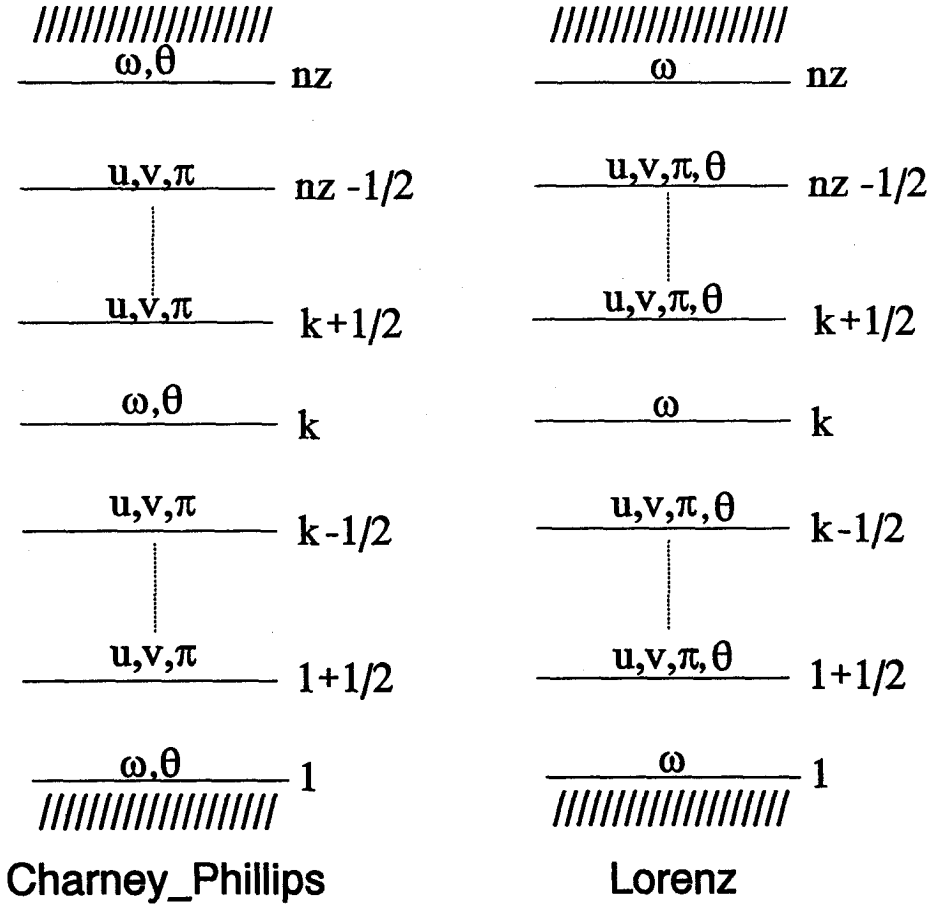

Fig. 4 Position of the variables of the Charney-Phillips and Lorenz grids. (π = Exner pressure).

terms treated implicitly, rather than extracting a constant coefficient problem in the usual way. The coefficients had to be selected to maximize the ellipticity of the pressure correction equation. In addition, accurate treatment of all the components of the pressure gradient term within the implicit step was found necessary to obtain satisfactory solutions over orography. In the two-dimensional problems solved in that paper it was sufficient to solve the variable coefficient elliptic equation by iterating a constant coefficient solver. However, this might not be adequate in a three-dimensional problem.

c *Non-hydrostatic integration schemes*

A number of atmospheric models have recently been extended to include non-hydrostatic effects. Techniques where a pressure-based coordinate is retained have

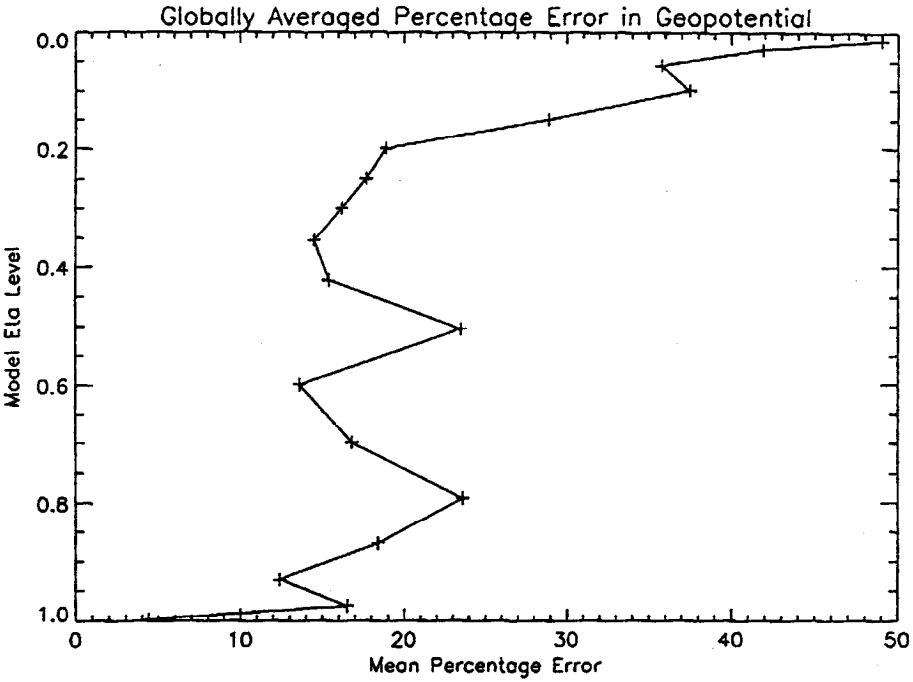

Fig. 5 Comparison of retransformed geopotential increment field with wind derived geopotential increment field. The original geopotential field is derived from non-surface wind observations. The percentage error is determined by dividing the rms difference between the two fields by the rms value of the original field, and multiplying by 100%. Note that a model eta level of 1 corresponds to the surface, and of zero to outer space.

been popular, because the conversion job is easier (Dudhia, 1993; Laprise, 1992). The 'unified' model currently uses a hybrid pressure-based coordinate from which the pressure at each level has to be recalculated every time step. Since it is more natural to use a height based vertical coordinate, especially if the full compressible Navier-Stokes equations are used and since pressure and height are then both available at all points, the interface to the physics routine does not need radical change to accommodate this. An area of difficulty, however, is the use of the two time-level schemes. In the unified model, a two time-level scheme is used with great advantage, as different time steps can easily be employed for different processes, and coupling the atmosphere to other models is also simpler because a single time-level of data provides a well-defined interface. Skamarock and Klemp (1992) demonstrated and analyzed instabilities in many two time level split schemes for the non-hydrostatic equations. Golding (1992) used such a scheme successfully, but found it necessary to use a basic state temperature profile in the semi-implicit method very close to the actual state. This would not be practical in a global model.

It is therefore proposed that a basic state profile is not used when selecting those parts of the equations to be treated implicitly. This requires the use of a variable coefficient solver for the implicit equations.

d *Implementation aspects*

Both requirements that the new scheme seeks to satisfy lead to the need to solve a variable coefficient elliptic equation. Efficient solution methods for these are therefore necessary. One of the most robust and efficient methods for use in computational fluid dynamics is considered to be the multigrid method. Application of this to meteorological problems is discussed by Fulton (1986). However, there are still doubts about its robustness for problems such as flow over orography, and other methods may yet prove superior.

The use of this type of semi-implicit method provides a way of satisfying the energy conservation requirement on the Charney-Phillips grid. Proof of energy conservation requires that the updates to the variables comprising the equation of state are calculated consistently. On the Charney-Phillips grid, the vertical staggering of the potential temperature from the pressure and density causes the difficulty. The solution is to generate the pressure correction equation by using an estimate of the vertically averaged potential temperature at the new time level calculated as

$$\overline{\theta^{n+1}}^z = \overline{\theta^n}^z + \underline{u} \cdot \overline{\nabla\theta}^z \tag{1}$$

rather than

$$\overline{\theta^{n+1}}^z = \overline{\theta^n}^z + \overline{\underline{u}^z \cdot \nabla\theta}^z \tag{2}$$

The update of θ using the corrected pressure and consequently corrected winds is made using the normal (semi-Lagrangian) advection.

4 Description of the proposed scheme

The fully compressible equations of motion are used, with a basic vertical coordinate r defining distance from the centre of the Earth, and a terrain following coordinate η derived from it taking values $\eta = 1$ at the upper boundary of the model and $\eta = 0$ at the Earth's surface. The equations are written in terms of a density ρ scaled by r^2. The equations take the following time-discretized forms

$$u^{n+1} - u_d^n + \Delta t\left[-2\Omega(\bar{v}^t \sin\phi - \bar{w}^t \cos\phi) + \frac{C_p\theta_v^n}{r\cos\phi}\left(\frac{\partial\bar{\Pi}^t}{\partial\lambda} - \frac{\partial\bar{\Pi}^t}{\partial r}\frac{\partial r}{\partial\lambda}\right)\right]$$

$$= \frac{1}{\rho}\frac{\partial\bar{\tau}_x^t}{\partial r} \tag{3}$$

$$v^{n+1} - v_d^n + \Delta t\left[2\Omega\bar{u}^t \sin\phi + \frac{C_p\theta_v^n}{r^n}\left(\frac{\partial\bar{\Pi}^t}{\partial\phi} - \frac{\partial\bar{\Pi}^t}{\partial r}\frac{\partial r}{\partial\phi}\right)\right] = \frac{1}{\rho}\frac{\partial\bar{\tau}_y^t}{\partial r} \tag{4}$$

$$w^{n+1} - w_d^n + \Delta t\left[-2\Omega u^n \cos\phi + \left(g\frac{(1+q_T)}{(1+q)}\right)^n + C_p\overline{\theta_v}^{t}\frac{\partial\bar{\Pi}^t}{\partial r}\right] = 0 \tag{5}$$

$$\rho_y^{n+1} - \rho_y^n + \frac{\Delta t}{\partial r/\partial\eta}\left[\frac{1}{\cos\phi}\frac{\partial}{\partial\lambda}\left(\frac{\rho_y}{r}\bar{u}^t\frac{\partial r}{\partial\eta}\right)\right.$$

$$\left. + \frac{1}{\cos\phi}\frac{\partial}{\partial\phi}\left(\frac{\rho_y}{r}\bar{v}^t\cos\phi\frac{\partial r}{\partial\eta}\right) + \frac{\partial}{\partial\eta}\left(\rho_y\overline{\dot{\eta}}^t\frac{\partial r}{\partial\eta}\right)\right] = 0 \tag{6}$$

$$\theta_L^{n+1} - \theta_{Ld}^n = \Delta t\left[\left(\frac{\theta}{TC_p}\right)Q + \frac{\kappa\theta\omega}{pTC_p}(L_c q_{CL} + (L_c + L_f)q_{CF})\right] \tag{7}$$

$$q_T^{n+1} - q_{Td}^n = S\Delta t \tag{8}$$

$$\Pi^{\frac{\kappa-1}{\kappa}}\theta_v\rho = \frac{p_0 r^2}{\kappa C_p} \tag{9}$$

Suffix d denotes the departure point for the semi-Lagrangian scheme and superscripts n and $n+1$ refer to time levels. The overbar indicates time averaging. The metric terms which would appear in the Eulerian form of the horizontal momentum equations are absorbed into the departure point calculation (Bates et al., 1990). Equation (9) is the equation of state. The notation is set out in Table 1. The implicit treatment of the advecting velocity and certain of the Coriolis terms is required to ensure conservation.

Solution of (3) and (9) as they stand would require coupled solution for all variables as three dimensional variables at the new time-level. This would be extremely expensive, and without better understanding of the structure of the equations, possibly ill-conditioned, resulting in failure of the integration scheme. The proposed method is to solve the implicit equations approximately using a predictor-corrector method, which can be thought of as using the first iteration only of an iterative method. The predictor step estimates corrections u', v' w', ρ', θ', q', p' using a subset of the terms treated implicitly in (3) to (9) chosen so that they can be reduced to a single three-dimensional equation which is strongly elliptic and therefore can be reliably solved. This also allows use of the form (1) instead of (2) for the estimate θ'. The terms used are the pressure gradient terms, including implicit treatment of the coefficient θ_v multiplying the pressure gradient term in the vertical velocity equation, the velocities in the continuity equation, a diagonal approximation to the boundary layer friction terms, the Coriolis terms, and the terms representing the

TABLE 1. Symbols used in equations

(r, λ, ϕ)	Spherical polar coordinates relative to centre of Earth
η	Terrain following scaled vertical coordinate
u, v, w	Velocity components
$\dot{\eta}$	$\frac{D\eta}{Dt}$
Ω	Earth's rotation rate
p, p_0	Pressure and reference value of pressure
Π	Exner pressure $\left(\frac{p}{p_0}\right)^{\kappa}$
C_p	Specific heat of dry air at constant pressure
κ	Gas constant over C_p
ω	$\frac{Dp}{Dt}$
ρ, ρ_y	Density of moist and dry air scaled by r^2
T	Temperature
θ	Potential temperature
θ_v	Virtual potential temperature
θ_L	Liquid water potential temperature
q	Specific humidity
q_T	Total water content
τ_x, τ_y	Horizontal components of turbulent stress

advection of the vertical component of vorticity. Further details are given in internal reports available from the authors.

The differences from the current unified model equations are

i) Use of the fully compressible non-hydrostatic equations, but, as with the existing unified model scheme, the vertical Coriolis terms are retained and the shallow atmosphere approximation is not used.

ii) Use of height as a vertical coordinate.

iii) No artificial horizontal diffusion, as a result of using monotone semi-Lagrangian advection.

5 Tests of the proposed scheme

The scheme is being tested on the full suite of shallow water test problems described by Williamson et al. (1992) and various published test problems which address the performance of the scheme in the vertical. We first describe results to test the proposed use of the Charney-Phillips vertical grid staggering. In order to take advantage of published results, these tests were carried out within the non-hydrostatic model of Golding (1992). This uses most of the features of our proposed integration scheme, except that it uses a fixed reference temperature profile in the semi-implicit integration scheme.

a *Eady wave test*

This is a simulation of the Eady-wave model of cyclogenesis in which a growing wave forms from a finite perturbation to a baroclinically unstable atmosphere. The

experiment is similar to that of Nakamura and Held (1989). Their results were obtained using a hydrostatic primitive equation model, and were chiefly concerned with the process of equilibriation which occurs after the magnitude of the wave peaks at around day 7. The process of equilibration is complex and in a recent paper (Nakamura, 1994), it is suggested that the details are dependent on the form of horizontal diffusion. Since a semi-Lagrangian model has no added diffusion (and different intrinsic diffusion associated with the interpolation scheme), we compare results only for the first seven days of the simulation.

The non-hydrostatic equations are solved in a vertical (x, z) cross section on an f-plane at 45°N. All the variables are periodic in x with the domain length equal to the wavelength of the initial disturbance. The basic state is the same as that in Williams (1967) and consists of vertically sheared zonal flow in thermal wind balance with potential temperature. The pressure field is in hydrostatic balance with the temperature. All fields are assumed independent of y (the north-south coordinate) except for the basic state potential temperature and pressure.

The domain size was 4000 km in length and 10 km deep. The grid lengths used in the simulation were 31.25 km in x and 240 m in z. The basic state satisfies $\frac{\partial \theta}{\partial y} = -10^{-5}$, $\frac{\partial \theta}{\partial z} = 3.9 \times 10^{-3}$, $f = 10^{-4}$. The perturbation to the basic state coincides with the fastest growing eigenmode, as in Williams (1967). A short time step of 100 s was required at the end of the evolution when the gradients and velocities associated with the wave were very large.

The solutions on the two vertical grids were very similar for the first five days, when the fields are quite smooth. Figure 6 compares the results after 6 and 6.25 days, which are illustrative of the differences during days 5 to 7. There is considerably more noise in the Lorenz grid solution, especially near the upper boundary. The vertical velocity results (not shown) show stronger gravity wave activity on the Lorenz grid just below the upper boundary. The increased gravity wave activity is typical of the Lorenz grid solutions throughout the latter stages of the evolution. By day 7 the solution on the Charney-Phillips grid is also beginning to suffer from noise. The results support those of Arakawa and Moorthi (1987), also showing that their conclusions apply to non-hydrostatic models.

b *Boundary layer treatment*

A possible disadvantage of the Charney-Phillips grid is the implementation of the boundary layer scheme. Since the velocities are held at different levels from the thermodynamic variables, extra interpolations are required in implementing most standard parametrization schemes. Tests have therefore been carried out to assess whether these interpolations degrade the simulations.

The boundary layer scheme tested is based on that used by Golding (1993). The scheme calculates a turbulent kinetic energy (TKE) with the shear $\partial u/\partial z$ and vertical stability $\partial \theta/\partial z$ acting as the main generating factors. The tests used the version of the scheme with prognostic and diagnostic TKE, only the latter is illustrated. On the Charney-Phillips grid, the vertical shear and vertical stability are

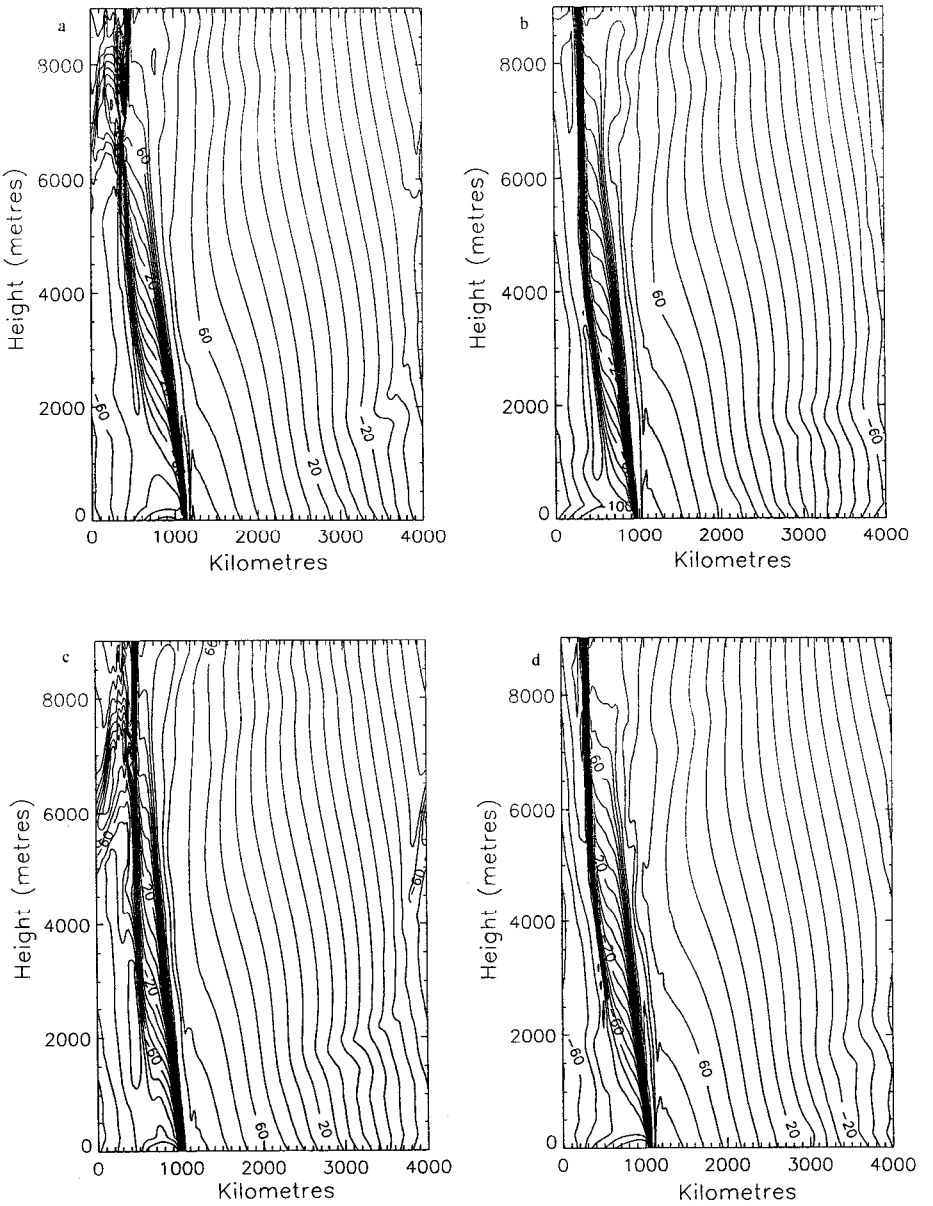

Fig. 6 y velocity components in Eady wave integration. a) Lorenz grid at 6 days, b) Charney-Phillips grid at 6 days, c) Lorenz grid at 6 1/4 days, d) Charney-Phillips grid at 6 1/4 days.

naturally calculated at different levels. There is a choice at which of these levels to hold the TKE, determining whether velocity or temperature variables have to be interpolated in calculating the generation terms. Both choices were tested.

The first experiment illustrated is a one-dimensional simulation of the evolution of the boundary layer at Wangara following data taken on 16 August 1967. This is a standard test bed for boundary layer parametrizations, e.g. Yamada and Mellor (1975), Golding (1993). Simulations using the Lorenz grid are compared with the two methods of implementation on the Charney-Phillips grid.

The integration is initialized at 0600 LST. Potential temperature, TKE, and u velocity were inspected at regular intervals up to 2400 LST, illustrated in Fig. 7. The experiment shows the response of the boundary layer as the solar heating of the land surface produces TKE and a subsequently well-mixed boundary layer. The land surface then cools and the TKE dies away, allowing a shallow inversion approximately 10 metres deep to form. At this point there is a little TKE above the immediate surface generated by wind shear.

All the integrations give similar results up to 1800 LST. After this time the Charney-Phillips integration which interpolates the velocity variables retains more TKE giving too much mixing and failure to form an inversion. The integration interpolating temperature variables gives similar results to the Lorenz grid.

A second experiment illustrates the interaction of the boundary layer scheme with the dynamics in a two-dimensional simulation. The simulation is of the development of fog at Perth (Western Australia) on 27 April 1990. The domain represents a cross section normal to the coast, with an idealized representation of the orography. The coast is 60 km from the western boundary, with 30 km of flat plain at 1 m above sea level to its east. This is terminated by a 10 km wide scarp rising linearly to a plateau at 300 m. The horizontal resolution used was 5 km. Experiments were performed using the vertical resolution of Golding (1993, Appendix 1). North-south derivatives are ignored except for a fixed pressure gradient term in the y-momentum equation. The synoptic situation and surface roughness and moisture availability are as described by Golding. The radiative forcing was, however, simplified to use constant prescribed day- and night-time heating rates.

The simulations are initiated at 1900 LST. Nine hours of simulated nocturnal cooling is represented by a fixed rate of downward radiative flux of 314 W m^{-2}. The downward radiative flux is then increased linearly over one hour to 1000 W m^{-2} at which it is held for a further two hours as a representation of dawn and daytime heating. Golding describes the nocturnal evolution as follows: 'Winds coming off the sea are approximately westerly with speed 8 m s^{-1}. The rough land surface rapidly decelerates the near-surface air allowing the surface temperature to drop. A highly turbulent boundary layer has developed on the scarp together with a weak easterly drainage flow that locally raises wind speed and temperatures and reduces humidity where it flows out onto the plain. These effects are diluted by surface cooling as it spreads onto the plain, but the enhanced shear generates turbulence. Between westerly winds from the sea and the easterly drainage flow, a stagnation

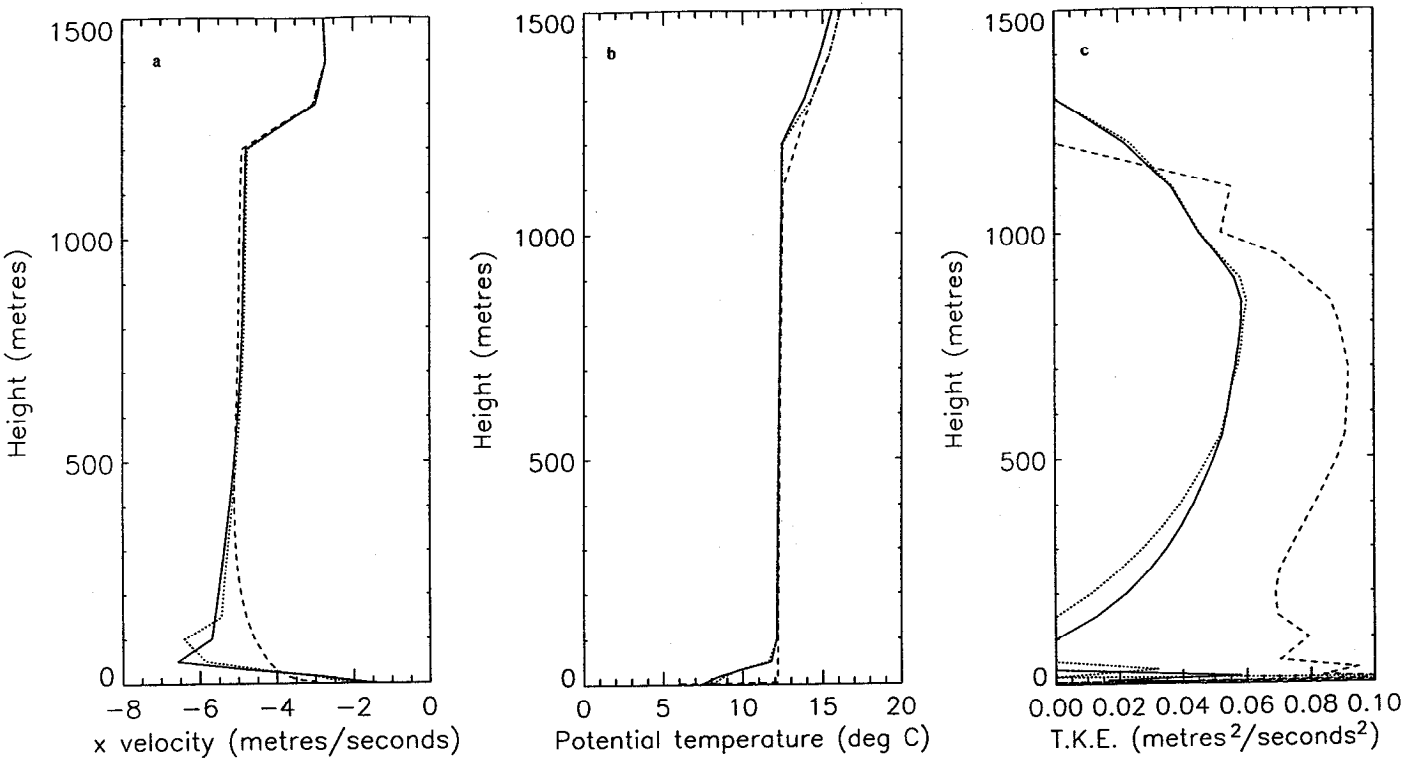

Fig. 7 Vertical profiles of: a) x-velocity, b) potential temperature, c) turbulent kinetic energy at 2400 LST. Charney-Phillips grid with velocity variables interpolated (dashed line), the Charney-Phillips grid with temperature variables interpolated (dotted line) and Lorenz grid (continuous line).

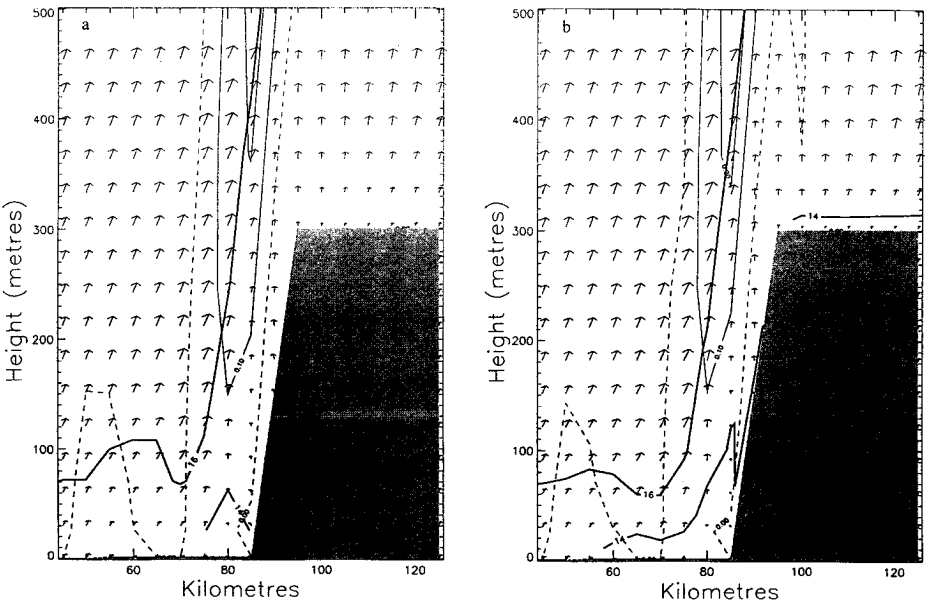

Fig. 8 Results from the Perth fog simulation experiment at 400 LST; a) Charney-Phillips grid, b) Lorenz grid. Horizontal wind velocity and direction (arrows), vertical velocity (light contours and zero contour dashed), potential temperature (heavy contours).

point has formed with associated weak uplift connected to the main scarp-driven ascent. This localized reduction in horizontal winds, and the associated drop in turbulent mixing, allow saturation to occur in the lowest model layers. At the same time, the upward motion associated with the convergent wind flow assists in deepening the saturated layer.'

Figure 8 shows the wind and potential temperature cross-sections using the Charney-Phillips grid with temperature variables interpolated and the Lorenz grid at 0400 LST. At this time the drainage flow is reaching a maximum. The differences are small. The area of descent is slightly greater if the Charney-Phillips grid is used. It is not possible to state which solution is preferable. A similar conclusion applies at other times. If the Charney-Phillips grid is used with momentum variables interpolated (not shown), there are considerable differences, including large vertical oscillations in the TKE. This is consistent with the results from the one-dimensional tests.

It is felt that these results show that the boundary layer simulation is not degraded by using the Charney-Phillips grid.

c *One dimensional behaviour of compressible model*

The proposed implementation of the integration scheme recommended in Section 3 uses a different way of constructing the semi-implicit scheme from that of Golding

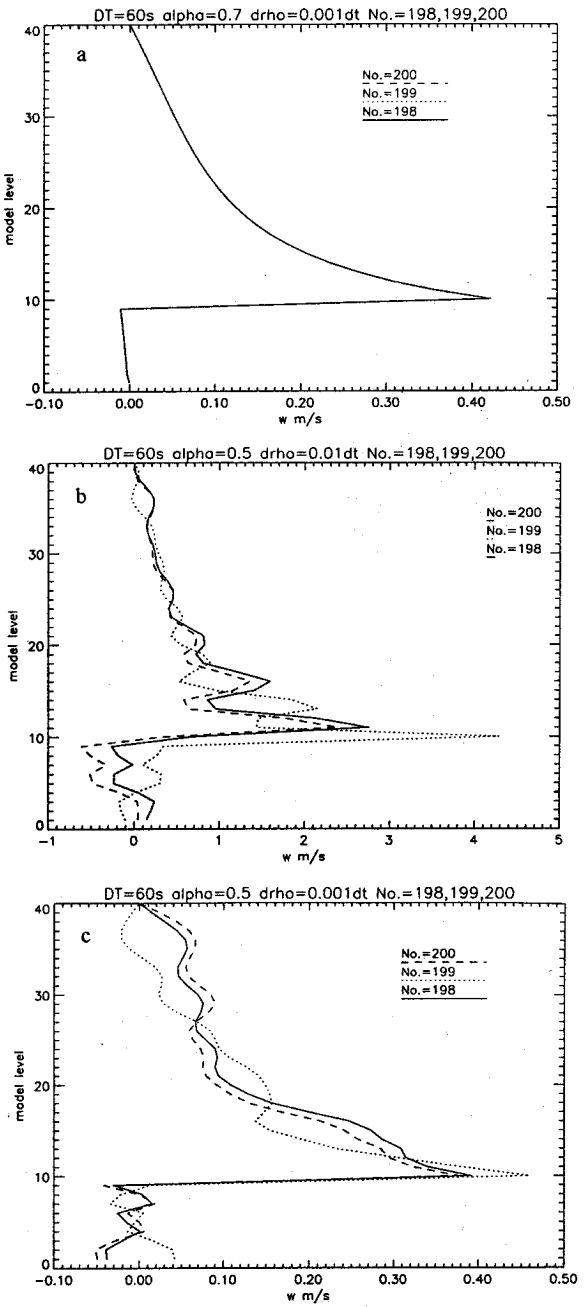

Fig. 9 Vertical velocity profiles in perturbed columns; (a) with backward implicit weighting, (b) no damping, (c) with initial perturbation 10 times larger. Superimposed curves are for successive time steps.

(1992), in particular working from a residual in the equation of state. The test described by Golding is thus repeated, in which perturbations to a vertical column of air 16 km high are simulated with a grid of 40 points and rigid upper and lower boundary conditions. The column is initially at rest in hydrostatic balance and is perturbed with a steady fractional mass source of 0.001 s^{-1} at the 10th point above the bottom. This source corresponds to major diabatic forcing. A 60 s time step was used for the integrations. The steady state response is an almost universally increasing pressure, with a slight gradient required to support the vertical motion required to redistribute the mass. On this are superposed the sound waves from the initial start-up. In the atmosphere the sound wave transients would not be of significant amplitude, and the open upper boundary condition would prevent resonance which is possible in this model.

Figures 9a) and b) show results comparable to Fig. 2 (right hand pair of profiles) of Golding (1992). The vertical velocity field is shown at three consecutive time steps. With centred implicit time differencing oscillations similar to those of Golding occur, but there is no tendency for them to amplify. With backward weighted time differencing ($\alpha = 0.7$) the transients disappear. Figure 9c) shows the results with centred time differencing using a mass source 10 times larger. There is again no unstable behaviour.

These results suggest that the basic structure of the time differencing scheme should be satisfactory.

6 Summary

We have presented a non-hydrostatic integration scheme which should be suitable for all applications of the unified model. Tests of some of the less usual aspects have been presented, giving satisfactory results. Further standard idealized tests are in progress and will be reported in due course.

References

ARAKAWA, A. and V.R. LAMB. 1977. Computational design of the basic dynamical processes of the UCLA general circulation model. In: *Methods in Comp. Phys.* Vol. **17**, Academic Press, pp. 174–265.

——— and S. MOORTHI. 1987. Baroclinic instability in vertically discrete systems. *J. Atmos. Sci.* **45**: 1688–1707.

BATES, J.R.; F.H.M. SEMAZZI, R.W. HIGGINS and S.R.M. BARROS. 1990. Integration of the shallow water equations on a sphere using a vector semi-Lagrangian scheme with a multigrid solver. *Mon. Weather Rev.* **118**: 1615–1627.

COURTIER, P. and J.-F. GELEYN. 1988. A global numerical weather prediction model with variable resolution: Application to shallow water equations. *Q.J.R. Meteorol. Soc.* **114**: 1321–1346.

CULLEN, M.J.P. 1989. Implicit finite difference methods for modelling discontinuous atmospheric flows. *J. Comp. Phys.* **81**: 319–348.

———. 1993. The unified forecast/climate model. *Meteorol. Mag.* **122**: 81–93.

——— and T. DAVIES. 1991. A conservative split-explicit scheme with fourth order horizontal advection. *Q.J.R. Meteorol. Soc.* **117**: 993–1002.

DUDHIA, J. 1993. A non-hydrostatic version of the Penn State-NCAR mesoscale model: validation tests and simulation of an Atlantic cyclone and cold front. *Mon. Weather Rev.* **121**: 1493–1513.

FULTON, S.R. 1986. Multigrid methods for elliptic

problems: a review. *Mon. Weather Rev.* **114**: 943–959.

GADD, A.J. 1978. A split-explicit scheme for numerical weather prediction. *Q.J.R. Meteorol. Soc.* **104**: 569–582.

GOLDING, B.W. 1992. An efficient non-hydrostatic forecast model. *Meteorol. Atmos. Phys.* **50**: 89–103.

———. 1993. A study of the influence of terrain on fog development. *Mon. Weather Rev.* **121**: 2529–2541.

LAPRISE, R. 1992. The Euler equations of motion with hydrostatic pressure as an independent variable. *Mon. Weather Rev.* **120**: 197–207.

LESLIE, L.M. and R.J. PURSER. 1992. A comparative study of the performance of various vertical discretisation schemes. *Meteorol. Atmos. Phys.* **50**: 61–73.

MORTON, K.W. and P.K. SWEBY. 1987. A comparison of flux limited difference methods and characteristic Galerkin methods for shock modelling. *J. Comp. Phys.* **73**: 203–230.

NAKAMURA, N. 1994. Nonlinear equilibriation of two-dimensional Eady waves: simulations with two-dimensional geostrophic momentum equations. *J. Atmos. Sci.* **51**: 1023–1035.

——— and I.M. HELD. 1989. Nonlinear equilibriation of two-dimensional Eady waves. *J. Atmos. Sci.* **46**: 3055–3064.

PRIESTLEY, A. 1993. A quasi conservative version of the semi-Lagrangian advection scheme. *Mon. Weather Rev.* **121**: 621–629.

SKAMAROCK, W.C. and J.B. KLEMP. 1992. The stability of time-split numerical methods for the hydrostatic and the non-hydrostatic elastic equations. *Mon. Weather Rev.* **120**: 2109–2127.

TANGUAY, M.; A. ROBERT and R. LAPRISE. 1990. A semi-implicit semi-Lagrangian fully compressible regional forecast model. *Mon. Weather Rev.* **118**: 1970–1980.

WHITE, A.A. and R.A. BROMLEY. 1995. Dynamically consistent, quasi-hydrostatic equations for global models with a complete representation of the Coriolis force. *Q.J.R. Meteorol. Soc.* **121**: 399–418.

WILLIAMS, R.T. 1967. Atmospheric frontogenesis: a numerical experiment. *J. Atmos. Sci.* **29**: 3–10.

WILLIAMSON, D.L.; J.B. DRAKE, J.J. HACK, R. JAKOB, and P.N. SWARTZRAUBER. 1992. A standard test set for numerical approximations to the shallow water equations in spherical geometry. *J. Comp. Phys.* **102**: 211–224.

——— and J.G. OLSON. 1994. Climate simulations with a semi-Lagrangian version of the NCAR community climate model. *Mon. Weather Rev.* **122**: 1594–1610.

YAMADA, T. and G.L. MELLOR. 1975. A simulation of the Wangara atmospheric boundary layer data. *J. Atmos. Sci.* **32**: 2309–2329.